Dynamic-Confidence-Level Chance-Constrained Voltage Control of Active Distribution Networks

Cheng Gong[1], Chenhui Lin[2*], Yunpeng Jiang[2], Guannan Wu[2], Wenchuan Wu[2], Yue Yang[3]
[1]*Tsinghua Shenzhen International Graduate School, Tsinghua University, Shenzhen, China*
[2]*Department of Electrical Engineering, Tsinghua University. Beijing, 100084, China*
[3]*School of Electrical Engineering and Automation, Hefei University of Technology, Hefei, China*

***Abstract*—With the rapid integration of renewable energy, the increasing penetration of photovoltaic (PV) stations in distribution networks has heightened grid volatility and uncertainty. While most existing studies address uncertainty using chance-constrained voltage control based on specific distribution assumptions, they insufficiently account for distributional shape. This paper proposes a chance-constrained control framework with dynamic quantiles. We first construct an accurate Gaussian Mixture Model (GMM) of PV outputs using a Conditional Gaussian Mixture Model (CGMM). Then, employing a risk-aware mechanism, we adapt the lower and upper quantiles of the chance constraints based on the kurtosis and skewness of distribution, thereby striking a balance between loss reduction and safety margins. Based on a modified IEEE 33-bus test system, we analyze the trade-off between operational risk and cost effectiveness across different loss levels and confidence levels. Numerical simulations demonstrate that the proposed method, which features dynamically adaptive confidence levels, achieves a superior balance between security and economy compared with conventional chance-constrained methods.**

***Index Terms*--dynamic quantiles; chance constraints; PV outputs; ADN voltage control**

I. Introduction

With the growing penetration of distributed renewable energy, active distribution networks (ADN) are increasingly exposed to uncertainty and randomness [1]. In particular, PV outputs can cause rapid variations in power flows, resulting in issues such as reverse power flow, increased network losses, and operational safety concerns. A primary consequence is a higher likelihood of voltage violations under excessive renewable injections, as widely reported in high-PV feeders. In such settings, deterministic formulations—built on perfect-forecast assumptions—are often inadequate, whereas chance-constrained control explicitly quantifies risk and curbs voltage violations under uncertainty [2].

Existing work can be grouped into four main streams. 1) Deterministic methods in [3-5] : The PV outputs and load demands are assumed to be fully known, with no randomness involved. The proposed model and methods are not applicable to ADN with a high proportion of renewable energy. 2) Gaussian distribution-based chance-constrained methods in [6-8]: The PV outputs are assumed to follow Gaussian distributions in the construction of chance-constrained formulations; however, the modeling errors introduced compromise system security. 3) Box/moment or fuzzy-set-based chance-constrained methods in [9-11]. Compared to the Gaussian assumption, these methods improve robustness, but still fail to capture the true distributions of PV outputs, which limits the system's operational safety. 4) Scenario enumeration based parametric assumptions in [12-15]. However, the scalability and solution quality degrade as the number of scenarios increases, making it difficult to balance the number of scenarios with the quality of the solutions.

To address the forementioned defects, we propose a shape-aware stochastic control framework for ADN with a high proportion of PV. CGMM leverages historical PV outputs together with PV forecasts to model the next time step, yielding a high-accuracy GMM of PV outputs. Uncertainty is then propagated through network sensitivity matrices to obtain GMMs for voltages and currents [16]. The GMMs for both voltage and current are generated, preserving their multimodality, skewness, and tail behavior, which directly influence constraint violations. Beyond fixed confidence levels, we extract kurtosis and skewness to adaptively determine the lower/upper probability levels, and embed these adaptive quantiles into deterministic counterparts of the chance constraints. The contributions of this paper are as follows.

- A method for adaptively adjusting confidence levels based on the distribution shape is proposed in this paper. We provide a principled mapping that expresses the upper/lower quantiles as functions of kurtosis and skewness, enabling risk-aware adjustments.
- A shape-preserving uncertainty propagation method is established in this paper. CGMM models PV output as a conditional GMM that captures multimodality. The sensitivity mapping propagates this distribution to voltages and currents while preserving higher-order features (such as skewness and heavy tails) that contribute to violations—thus avoiding the information loss inherent in mean–variance models.

979-8-3315-8138-1

The remainder of the paper is organized as follows. Section II details the ADN voltage control model and receding-horizon setup. Section III presents the adaptive confidence-level pipeline. Section IV reports the case study on quantile computation and comparative results. Section V summarizes the conclusion.

II. ADN Voltage Control Model

A. ADN Voltage Control Model

The following section presents the ADN voltage control model, which is formulated with the objective of minimizing network losses and photovoltaic curtailment.

$$min \sum_{(i,j)\in\Omega_L} r_{ij}L_{ij,t} + \sum_{j\in\mathcal{N}} P_{j,t}^{pvc} \quad (1)$$

Subject to:

$$\sum_{m:j\to m} P_{jm,t} - \left(P_{ij,t} - r_{ij}L_{ij,t}\right) = P_{j,t}^{pv} - P_{j,t}^{pvc} - P_{j,t}^{d}, \forall j \in \Omega_B \quad (2)$$

$$\sum_{m:j\to m} Q_{jm} - \left(Q_{ij} - x_{ij}L_{ij,t}\right) = q_{j,t}^{pv} - q_{j,t}^{d}, \forall j \in \Omega_B \quad (3)$$

$$V_{i,t}^2 - V_{j,t}^2 = 2(R_{ij}P_{ij,t} + X_{ij}Q_{ij,t}), \forall (i,j) \in \Omega_L \quad (4)$$

$$I_{ij}^{min} \le \tilde{I}_{ij}^{t} \le I_{ij}^{max}, \forall (i,j) \in \Omega_L \quad (5)$$

$$V_i^{min} \le \tilde{V}_i^{t} \le V_i^{max}, \forall \mathrm{i} \in \Omega_B \quad (6)$$

$$L_{ij,t} = I_{ij,t}^2, \forall (i,j) \in \Omega_L \quad (7)$$

$$I_{ij,t} = \frac{\sqrt{(P_{ij,t})^2 + (Q_{ij,t})^2}}{V_{i,t}}, \forall (i,j) \in \Omega_L \quad (8)$$

$$0 \le P_{0,t} \le P_{0,max} \quad (9)$$

$$0 \le Q_{0,t} \le Q_{0,max} \quad (10)$$

The objective function (1) of the distribution-network model aims to minimize total losses: the first term represents the aggregate line losses, while the second term quantifies PV curtailment. Constraints (2)-(3) enforce active and reactive power balance. Constraint (4) captures the physical relationship between voltage changes and power flows. Constraint (5) bounds branch currents. Constraint (6) restricts nodal voltages. Constraint (7) states that $L_{ij,t}$ equals the square of the branch current $I_{ij,t}$. Constraint (8) provides the calculation formula for branch currents. Constraint (9) limits the active power purchased from the upstream grid. Constraint (10) limits the reactive power purchased from the upstream grid.

B. PV Output Model

PV inverters have the capability to regulate the power factor and inherently provide a certain amount of reactive power support.

$$0 \le P_{j,t}^{pvc} \le P_{j,t}^{pv} \quad (11)$$

$$q_{pv,j}^{min} \le q_{j,t}^{pv} \le q_{pv,j}^{max} \quad (12)$$

$$\sqrt{(P_{j,t}^{pvc})^2 + (q_{j,t}^{pv})^2} \le S_{i,pv} \quad (13)$$

where constraint (11) is the active-power limit of the PV, constraint (12) defines its reactive-power regulation capability, and constraint (13) imposes the apparent-power capacity limit. Together these three constraints constitute the mathematical model of a PV power station.

C. Stochastic Receding Horizon Control Framework

Figure 1 presents the detailed framework of the proposed control method, which iteratively integrates dynamic-quantile adjustment into active-distribution-network voltage control. First, the overall control horizon T_{max} is defined, representing the entire time span over which the control is performed. The system is initialized at $t = 0$; based on the PV data at time t, a probabilistic forecast of PV outputs for time $t + 1$ is generated. Next, a sensitivity matrix maps the PV-output distribution into nodal-voltage and branch-current distributions. The kurtosis and skewness of these distributions are then computed, and the dynamic lower and upper quantiles are derived accordingly.

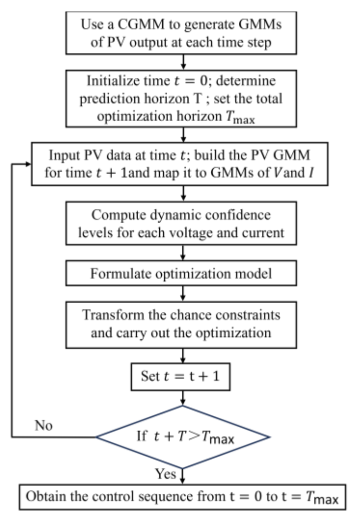

Figure 1. Control flow chart

By integrating CGMM-based probabilistic PV forecasting, dynamic confidence-level calculation via sensitivity analysis, and iterative active-distribution-network voltage control, the proposed pipeline effectively copes with PV-output uncertainty and delivers accurate, adaptive control strategies for distribution networks at a controllable computational cost.

It is worth emphasizing that the key steps—CGMM-based probabilistic forecasting, sensitivity-based distribution mapping, and dynamic confidence-level updating—are all designed to handle the stochastic nature of PV outputs. The

979-8-3315-8138-1

iterative control loop guarantees that control actions are refreshed in real time with the latest PV data, enhancing the adaptability and robustness of network operation.

III. Dynamic Confidence Level Generation

A. GMM Model for PV Output

GMM can accurately represent the power output of renewable energy. To better exploit contextual information, we construct the PV output distribution using CGMM, which allows more features to be incorporated as inputs.

Specifically, we divide each day into 96 time steps and apply temporal encoding to both historical actual measurements and forecast data. The temporal encoding together with the forecast for the next time step serve as conditional inputs. We then retrieve historical PV actual outputs that match these conditions as sample points for model fitting, thereby constructing a conditional probabilistic model of PV outputs.

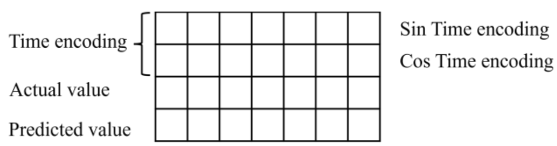

Figure 2. Temporal encoding of historical data

B. GMM Model for Voltage and Current

In an active distribution network, the nodal voltages and branch currents follow as:

$$y = A\xi + Bx + c \tag{14}$$

where y denotes the vector of node voltages or branch currents, ξ is the random PV-output vector, x is the vector of control decision variables, A is the sensitivity matrix of y with respect to ξ, B is the sensitivity matrix of y with respect to x, and c represents the baseline operating point when ξ and x are set to zero. Take constraint (6) as example, y represents $\tilde{V}_i^t$, ξ represents the Predicted PV output $P_{j,t}^{pv}$, x represents the PV curtailment $P_{j,t}^{pvc}$ and PV reactive power $q_{j,t}^{pv}$. c is the baseline voltage when both PV output and decision variables are zero. A and B are the sensitivity matrices of voltage with respect to PV output, curtailment, and reactive power.

Based on the established probability distribution of ξ, the affine mapping $A\xi$ yields GMM distributions for the mapped quantities—node voltages and branch currents. The corresponding cumulative distribution function can be written as follows:

$$CDF_{\xi}(x) = \sum_{k=1}^{K} \pi_k \Phi\left(\frac{x-\mu_j}{\sigma_j}\right) \tag{15}$$

$$\pi_k \geq 0, k = 1,2,\ldots,\mathrm{K} \tag{16}$$

$$\sum_{k=1}^{K} \pi_k = 1 \tag{17}$$

where K is the number of mixture components; $CDF_{\xi}(x)$ is the cumulative distribution function of the GMM; π_k is the mixing weight of the k-th Gaussian component.

C. Confidence Level Calculation

Existing chance-constrained control methods typically rely on symmetric quantiles—such as the 2.5 % and 97.5 % points—thereby ignoring the fact that real-world PV-output distributions are usually skewed. When the distribution is left-skewed, the downside tail risk is higher, so the lower confidence bound should be shifted further to the left. Conversely, when the distribution is right-skewed, the upper bound should be adjusted similarly [17]. Higher kurtosis implies fatter tails and a greater probability of extreme events, so both quantiles should be moved inward to increase the safety margin in the tails [18].The skewness and kurtosis are computed as follows:

$$\mu = \sum_{k=1}^{K} \pi_k \mu_k \tag{18}$$

$$\sigma^2 = \sum_{k=1}^{K} \pi_k [\sigma_k^2 + (\mu_k - \mu)^2] \tag{19}$$

$$m_3 = \sum_{k=1}^{K} \pi_k \left[\delta_k^3 + 3\delta_k \sigma_k^2\right] \tag{20}$$

$$\begin{aligned} m_4 = \sum_{k=1}^{K} \pi_k [&(\mu_k - \mu)^4 \\ &+ 6(\mu_k - \mu)^2 \sigma_k^2 + 3\sigma_k^4] \end{aligned} \tag{21}$$

$$\gamma_1 = \frac{m_3}{\sigma^3} \tag{22}$$

$$\gamma_2 = \frac{m_4}{\sigma^4} - 3 \tag{23}$$

where K is the number of mixture components; $\pi_k \in [0,1]$ is the mixing weight of the k-th component; μ_k is the mean of the k-th Gaussian component; σ_k^2 is its variance; μ and σ^2 are the overall mean and variance of the mixture; δ_k is the component-mean offset from the global mean; m_3 is the third central moment; m_4 is the fourth central moment; γ_1 is the skewness ; and γ_2 is the excess kurtosis. With γ_1 and γ_2 in hand, the upper and lower quantiles can be computed directly.

$$\begin{aligned} \alpha_{low} &= \alpha_0^{low} - \beta_k max(k-3,0) + \beta_s s \\ \alpha_{up} &= \alpha_0^{up} + \beta_k max(k-3,0) + \beta_s s \end{aligned} \tag{24}$$

Where α_0^{low} and α_0^{up} are the baseline confidence levels; β_k is the kurtosis-adjustment coefficient; β_s is the skewness-adjustment coefficient

D. Chance-Constraint Reformulation

Chance-constrained methods typically convert hard safety limits (such as voltage and current bounds) into probabilistic

979-8-3315-8138-1

form, requiring these limits to be satisfied with a specified probability [19]. The generic form is as follows:

$$y_i^{min} \le \tilde{y}_i^t \le y_i^{max} \tag{25}$$

$$\Pr\{y_i^{min} \le \tilde{y}_i^t \le y_i^{max}\} \ge 1-\alpha \tag{26}$$

$$\Pr\{y_i^{min} \le \tilde{y}_i^t\} \ge 1-\alpha_{low} \tag{27}$$

$$\Pr\{\tilde{y}_i^t \le y_i^{max}\} \ge 1-\alpha_{\mathrm{up}} \tag{28}$$

$$\hat{y}_{i,\alpha_{\mathrm{low}}}^t \le \tilde{y}_i^t \tag{29}$$

$$\tilde{y}_i^t \le \hat{y}_{i,\alpha_{\mathrm{up}}}^t \tag{30}$$

Based on equations (25) and (26), constraints (5) and (6) can be transformed into the chance-constrained form as shown in equation (26). Since the dynamic confidence levels are asymmetric, this is further expressed in the form of equations (27) and (28). With the voltage and current expressions derived from equation (14), the lower and upper quantiles $\hat{y}_{i,\alpha_{\mathrm{up}}}^t$ and $\hat{y}_{i,\alpha_{\mathrm{low}}}^t$ can be computed. Constraints (27) and (28) are equivalently transformed into constraints (29) and (30).

IV. Case Study

A. System Structure

A modified three-phase 33-bus, 12.66 kV ADN is employed to validate the proposed chance-constrained voltage control with adaptive confidence levels; its single-line diagram is given in Figure 3. Seven PV stations are installed at the locations indicated. The PV outputs are taken from the "ARPA-E PERFORM Dataset" provided by the U.S. National Renewable Energy Laboratory and scaled by an appropriate factor.

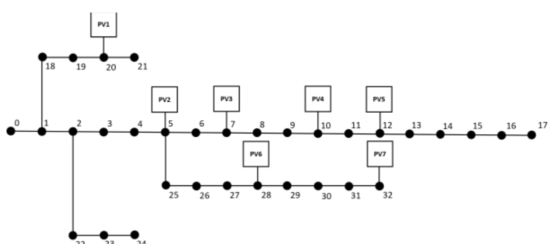

Figure 3. Network of the modified 33-bus distribution system

The overall horizon $T_{\max}$ is 96, with a time step of 15 minutes, optimizing over a 24-hour period. Pre-set voltage and current limits are [0.95, 1.05] p.u.; the skewness influence coefficient on the confidence level is set to $\beta_s = 0.01$, and the kurtosis influence coefficient on the confidence-interval length is $\beta_k = 0.02$. Loads follow the IEEE 33-bus benchmark and are normalized according to the daily load curve. Under this scenario, the effectiveness and robustness of the proposed adaptive-confidence-level chance-constrained method are clearly demonstrated.

B. PV Output Modeling Performance

This section evaluates the PV probabilistic modeling performance of the CGMM on historical data. The CGMM uses the forecasted PV value for the next time step, along with time encoding, as conditional inputs. It then searches for similar points in the historical data to serve as sample points. The Expectation-Maximization (E-M) algorithm is applied to fit a GMM to these sample points, resulting in a probabilistic distribution of PV output.

Below, we present the probability distribution plots of PV output for two PV stations at a specific time point, established using the CGMM.

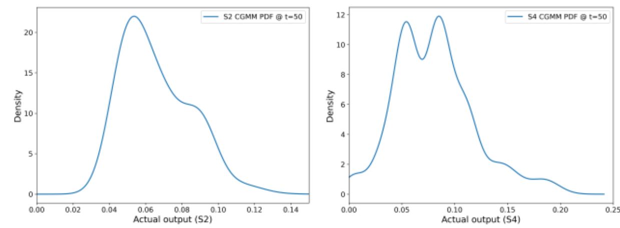

Figure 4. GMM plot of PV outputs of two PV stations

Figure 4 shows that the outputs of these two PV stations exhibit a right-skewed distribution, with higher probabilities and risks of exceeding the upper limits on the right side. The tail of the output distribution for the PV station on the right is thicker compared to that of the station on the left, indicating that the risk of exceeding the limits on both sides is generally higher for the PV station on the right. Additionally, the output distribution for the PV station on the right shows a multi-modal feature, indicating greater volatility in the output and a higher level of risk. This station, therefore, requires a larger safety margin. These findings demonstrate that the CGMM accurately captures the asymmetric uncertainties of PV outputs.

C. Quantile Computation Results

Based on the sensitivity-coefficient matrix, the PV-output GMM is mapped to nodal voltages and branch current. Then, the corresponding lower and upper quantiles are computed for each bus voltage and line current. To avoid over-aggressive or over-conservative limits, α_{low} is bounded below by 0.01 and α_{up} above by 0.99. The partial resulting voltages for the 5th period are listed below:

TABLE I. Upper/Low Voltage Quantiles of Selected Buses

Node number	α_{low}	α_{up}
1	0.01922008	0.98691169
2	0.02112902	0.99
3	0.02193913	0.99
4	0.02251966	0.99
5	0.0232954	0.99
6	0.02337676	0.99
7	0.0236453	0.99
8	0.02339054	0.98966875
9	0.02308856	0.98833804
10	0.02302839	0.98809809

TABLE I reports results for a subset of buses. Consistent with the right-skewed PV distribution at this time, the right-tail (over-voltage) risk is higher. Accordingly, the solved upper confidence levels are relatively conservative (e.g., $\alpha_{\mathrm{up}} \approx$

0.986–0.99), while the lower confidence levels are more aggressive (e.g., $\alpha_{\text{low}} \approx 0.019–0.024$). This asymmetric allocation of probability mass hedges the high-risk tail without being overly conservative on the low-risk side, thereby balancing security and economy.

D. Voltage Control Results Comparison

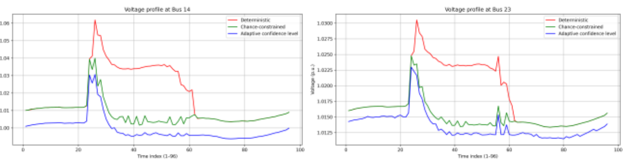

Figure 5. Voltage Magnitude Profiles over 96 Time Steps

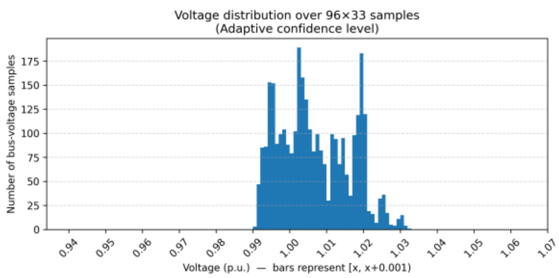

Figure 6. Voltage distribution over 96 Time Steps

This study uses the predicted PV probability distribution for 96 time steps to calculate decision variables, which are then applied to actual PV output scenarios for the next time step. The results are shown in Figure 5 and Figure 6. Figure 5 demonstrates that the deterministic voltage control struggles with the uncertainty of PV outputs, while both chance-constrained and dynamic confidence level chance-constrained voltage control shows much better performance, with the latter offering superior voltage control. This is due to the more conservative upper quantile selection in dynamic confidence level voltage control, which is better suited to handle skewed distributions. Figure 6 highlights that, under dynamic confidence Level voltage control, voltage violations were almost nonexistent over the 96-time-step period. This suggests that the method proposed in this paper has certain value for optimizing power systems with distributed generation.

V. CONCLUSION

An adaptive confidence level chance-constrained voltage control method is proposed. A CGMM-based PV output modeling method is introduced. Taking the modified IEEE 33-bus system as a case study, this paper compares deterministic voltage control, chance-constrained voltage control, and the proposed method. The case study shows that the proposed approach achieves better voltage control performance in distribution networks with distributed generation.

ACKNOWLEDGMENT

This work was supported in part by the National Natural Science Foundation of China (52307101, U24B6009, 52321004), and in part by the Beijing Natural Science Foundation (L243003), and in part by the Young Elite Scientists Sponsorship Program by CAST under Grant 2023QNRC001. (Corresponding author: Chenhui Lin).

REFERENCES

[1] X. Fu and Y. Zhou, “Collaborative optimization of PV greenhouses and clean energy systems in rural areas,” IEEE Trans. Sustain. Energy, vol. 14, no. 1, pp. 642–656, Jan. 2023.

[2] D. Lee, S. Park, and B. Lee, “Chance-constrained optimization for active distribution network operation considering virtual power lines,” *Electric Power Systems Research*, vol. 223, art. 109606, 2023.

[3] F. A. Chacra, P. Bastard, G. Fleury, and R. Clavreul, “Impact of energy storage costs on economical performance in a distribution substation,” IEEE Trans. Power Syst., vol. 20, no. 2, pp. 684–691, May 2005.

[4] G. Celli, S. Mocci, F. Pilo, and M. Loddo, “Optimal integration of energy storage in distribution networks,” in Proc. IEEE Conf. PowerTech, Bucharest, Romania, Jun. 2009, pp. 1–7.

[5] C. Thrampoulidis, S. Bose, and B. Hassibi, “Optimal placement of distributed energy storage in power networks,” IEEE Trans. Autom. Control, vol. 61, no. 2, pp. 416–429, Feb. 2016.

[6] Y. Cao, W. Wei, S. Mei, M. Shafie-khah, and J. P. S. Catalão, “Analyzing and quantifying the intrinsic distributional robustness of CVaR reformulation for chance-constrained stochastic programs,” IEEE Trans. Power Syst., vol. 35, no. 6, pp. 4908–4911, Nov. 2020.

[7] B. Tong, L. Zhang, G. Li, B. Zhang, F. Xie, and W. Tang, “An overvoltage-averse model for renewable-rich AC/DC distribution networks considering the sensitivity of voltage violation probability,” IEEE Trans. Sustain. Energy, vol. 16, no. 1, pp. 613–626, Jan. 2025.

[8] Z. Ding, X. Huang, Z. Liu, and Z. Zhang, “A two-level scheduling algorithm for battery systems and load tap changers coordination in distribution networks,” IEEE Trans. Power Deliv., vol. 37, no. 4, pp. 3027–3037, Aug. 2022.

[9] Z. Shi, H. Liang, S. Huang, and V. Dinavahi, “Distributionally robust chance-constrained energy management for islanded microgrids,” IEEE Trans. Smart Grid, vol. 10, no. 2, pp. 2234–2244, Mar. 2019.

[10] C. Han, R. R. Rao, and S. Cho, “Stochastic operation of multi-terminal soft open points in distribution networks with distributionally robust chance-constrained optimization,” IEEE Trans. Sustain. Energy, vol. 16, no. 1, pp. 81–94, Jan. 2025.

[11] J. H. Duan, J. J. Chen, F. W. Liu, P. H. Jiao, and B. Y. Xu, “Credibility theory to handle uncertain renewable energy: A fuzzy chance constrained AC optimal power flow,” Electr. Power Syst. Res., vol. 223, Art. no. 109550, 2023.

[12] M. Ding and X. Wu, “Three-phase probabilistic power flow in distribution system with grid-connected photovoltaic systems,” in Proc. IEEE APPEEC, Shanghai, China, Mar. 2012, pp. 1–6.

[13] S. S. Al Kaabi, H. H. Zeineldin, and V. Khadkikar, “Planning active distribution networks considering multi-DG configurations,” IEEE Trans. Power Syst., vol. 29, no. 2, pp. 785–793, Mar. 2014.

[14] S. Huang, J. Xiao, J. F. Pekny, G. V. Reklaitis, and A. L. Liu, “Quantifying system-level benefits from distributed solar and energy storage,” J. Energy Eng., vol. 138, no. 2, pp. 33–42, Jun. 2012.

[15] C. Abbey and G. Joos, “A stochastic optimization approach to rating of energy storage systems in wind-diesel isolated grids,” IEEE Trans. Power Syst., vol. 24, no. 1, pp. 418–426, Feb. 2009.

[16] W. Yin, "Models and applications of stochastic programming with decision-dependent uncertainty in power systems: A review," *IET Renewable Power Generation*, vol. 18, no. 14, pp. 2819-2834, Oct. 2024.

[17] M. Kipp and C. Koziol, “Tail risk management and the skewness premium,” J. Asset Manag., vol. 23, no. 6, pp. 534–546, Sep. 2022.

[18] X. Liu, “On tail fatness of macroeconomic dynamics,” J. Macroecon., vol. 62, Art. no. 103154, Dec. 2019

[19] T. Huang, Y. Sun, J. Hao, C. Sun, and C. Liu, "A distributed peer-to-peer energy trading model in integrated electric–thermal systems," *IET Renewable Power Generation*, vol. 18, no. 15, pp. 3188–3203, Nov. 2024.

979-8-3315-8138-1